World Academy of Science, Engineering and Technology
International Journal of Mathematical and Computational Sciences
Vol:2, No:9, 2008

# Analytical Analysis of Image Representation by Their Discrete Wavelet Transform

R. M. Farouk



***Abstract*—**In this paper, we present an analytical analysis of the representation of images as the magnitudes of their transform with the discrete wavelets. Such a representation plays as a model for complex cells in the early stage of visual processing and of high technical usefulness for image understanding, because it makes the representation insensitive to small local shifts. We found that if the signals are band limited and of zero mean, then reconstruction from the magnitudes is unique up to the sign for almost all signals. We also present an iterative reconstruction algorithm which yields very good reconstruction up to the sign minor numerical errors in the very low frequencies.

***Keywords*—**Wavelets, Image processing signal processing, Image reconstruction

## I. Introduction

THE early stage of processing of visual stimuli in the cortex is constituted by simple and complex cells in V1. Simple cell responses are modeled to considerable accuracy by linear convolution with Gabor functions [5,1]. Pairs of cells differing in phase by 90 degrees are frequently found [6]. Complex cells differ from simple cells by showing less specificity concerning the position of the stimulus. Their responses are well modeled by the magnitudes of the Gabor filter responses. Although the properties of these cells are more complicated, especially concerning temporal behavior, this functional description remains a good approximation to the cell responses.

We focus here on Gabor functions as an adjustable compromise between pixel representation and Fourier components. They seem to be implemented in the first stages of processing in the visual cortex of higher vertebrates, as the receptive fields of the so called simple cells can be described to some accuracy as Gabor functions [5,1]. There is also evidence that the magnitudes of Gabor filter responses are calculated by another set of cells called complex cells [7].

The simplest model for these findings is that simple cell responses are calculated from the image intensities by a feed-forward neural net, and that complex cells build on their information by another feed-forward net. The complex cells, in turn, can be combined to more complicated feature detectors such as corner detectors [8].

R. M. Farouk is with the Mathematics Department, Faculty of Science, Zagazig University, Egypt. E-mail rmfarouk1@yahoo.com

They have also proven useful for higher image understanding tasks such as texture classification [9], recognition of faces, vehicles [10], and others. The deeper reason for this is that the magnitude operation introduces some local shift invariance in the sense that under small shifts in the image. The Gabor magnitudes are more robust than full complex valued responses, because they are much smoother. This robustness is crucial for recognition systems, which have to cope with small local deformations. As a practical consequence, similarity landscapes between local features are smoother if magnitudes are used, which makes matching faster and less prone to local maxima [2,11]. If the Gabor functions are arranged into a wavelet transform and the sampling is dense enough then the original image can be recovered from the transform values with arbitrary quality (except for DC-value). Given the useful properties of the magnitudes of the Gabor transform an important theoretical question is how much image information can be recovered from that.

There are many results on the reconstruction of images from localized phase [13], and they show convincingly that localized phase in more useful than global Fourier phase. There seems to be general argument that reconstruction from phase is similar than reconstruction from local magnitude.

In this paper, we present a proof that, given appropriate transform parameters and band limitation, no image information is lost beside the DC-value of the image and a global sign. The proof uses techniques from Hayes and applies to all images except a possible subset of measure zero. The extension to localized Fourier transforms such as Gabor wavelets has not been shown before.

The practical importance of reconstruction from Gabor magnitudes seems quite limited. For the visual system, it is clearly not a problem because the simple cell information is readily available. The importance of our results lies on the theoretical analysis of the effects of the nonlinearity introduced by the magnitudes. We demonstrate that, on the one hand, the resulting representation shows invariance under small shifts, and on the other hand, not more information is lost than by sub-sampling by factor two, the global sign and DC value.

## II. Gabor Wavelets Transform

For the analysis of signal properties at various scales the wavelet transform is in wide use. The signal is projected onto a family of wavelet functions, which are derived from a single

mother wavelet by translation $\vec{x}_0$, rotation with matrix $R(\theta)$, and scaling by of 2-dimension signal $I(\vec{x})$ plane:

$$W_t(\vec{x}_0, s, \theta) = \frac{1}{s}\int_{R^2} I(\vec{x})\psi^*[\frac{1}{s}R(\theta)(\vec{x}-\vec{x}_0)]d^2x \quad (1)$$

The mother wavelet (and consequently, all wavelets) must satisfy the admissibility condition [3]:

$$0 < C = 4\pi^2 \int d^2\omega \frac{|\hat{\psi}|^2}{\|\omega\|^2} < \infty \quad (2)$$

Consequently the wavelets must have zero DC-value $\hat{\psi}(0) = 0$ and decay sufficiently quickly for increasing $|\omega|$. This condition, together with implementing the translations of wavelets as convolutions means that wavelets are band pass functions.

For modeling biological properties as well as to fulfill admissibility, standard Gabor functions are modified by term that removes their DC-value, turning the real and imaginary part into a strict matched filter pair. We let

$$\Psi(\vec{x}) = \frac{1}{\sigma_\nu}\exp\left(-\frac{1}{2}\|S_{\sigma,\nu}\vec{x}\|^2\left\{\exp(ix^T\vec{e}_1) - \exp\left(-\frac{\sigma^2}{2}\right)\right\}\right) \quad (3)$$

Consequently its Fourier transform is

$$\hat{\Psi}(\vec{\omega}) = \exp\left(-\frac{1}{2}\|S_{\sigma,\nu}^{-1}(\vec{\omega}-\vec{e}_1)\|^2\right) - \exp\left(-\frac{1}{2}\|S_{\sigma,\nu}^{-1}\omega\|^2\right) + \sigma^2 \quad (4)$$

In these equations the diagonal matrix

$S_{\sigma,\nu} = Diag\left(\frac{1}{\sigma}, \frac{1}{\nu}\right)$ controls the shape of the elliptical Gaussian relative to the wavelength.

## III. SAMPLING

In this section, we switch from continuous functions to discretely sampled images of $N \times N$ pixels. This lattice is denoted by $S_{\vec{N}}$, the sampling interval for images and translation space by $\hbar$. To avoid confusion, we use three different symbols for the different Fourier transforms: the continuous one (FT) is defined by:

$$\hat{I}(\vec{\omega}) = \frac{1}{2\pi}\int_{R^2} I(\vec{x})\exp(-i\vec{x}^T\vec{\omega})d^2x, \vec{\omega} \in R^2 \quad (5)$$

the 2-D equivalent of Fourier series is defined by

$$\hat{I}(\vec{v}) = \frac{1}{2\pi}\sum_{\vec{n}\in Z^2} I(\vec{n})\exp(-i\vec{v}^T\vec{n}), \vec{v} \in U^2 \quad (6)$$

and the completely discretized and finite version (DFT) is given by:

$$\hat{I}(\vec{\rho}) = \frac{1}{\sqrt{N_1 N_2}}\sum_{n\in S_{\vec{N}}} I(\vec{n})\exp(-i\pi\vec{\rho}\vec{n}^T), \vec{\rho} \in S_{\vec{N}} \quad (7)$$

For simplification, we also use normalized DFT coordinates $\vec{\rho}(\frac{\rho_1}{N_1}, \frac{\rho_2}{N_2})^T$ after some simplification, the final discretization of wavelet families in both spatial and frequency domain takes the form

$$\psi_{\vec{n}_0,m,l}(\vec{n}) = a_{\min}^{-1}a_0^{-m}\psi\left(a_{\min}^{-1}a_0^{-m}R(\frac{2\pi l}{L})\hbar(\vec{n}-\vec{n}_0)\right) \quad (8)$$

And their Fourier transform is given by:

$$\hat{\psi}_{\vec{n}_0,m,l}(\vec{\rho}) = \frac{2\pi a_{\min}a_0^{-m}}{\sqrt{N_1N_2\hbar}}\hat{\psi}\left(a_{\min}a_0^m R(\frac{2\pi l}{L})\frac{2\pi}{L}\vec{\rho}\right)\exp(2\pi\vec{n}_0^T\vec{\rho}) \quad (9)$$

Now, the discrete Gabor wavelet transform can be computed in either domain by the inner product

$$I(\vec{n}_0, m, l) = \sum_{\vec{n}\in S_{\vec{N}}} I(\vec{n})\psi^*_{\vec{n}_0,m,l}(\vec{n})$$
$$\ldots\ldots\ldots\ldots = \sum \hat{I}(\vec{\rho})\hat{\psi}^*_{\vec{n}_0,m,l}(\vec{\rho}) \quad (10)$$

and the inverse wavelet transform becomes

$$\hat{I}(\vec{\rho}) = \frac{\hbar^4}{4\pi^2}Y_0^{-1}(\vec{\rho})\sum_{\vec{n}_0\in S_{\vec{N}}}\sum_{m=0}^{M-1}\sum_{l=0}^{L-1} a_{\min}^{-2}a_0^{-2m}I(\vec{n}_0,m,l)\hat{\psi}_{\vec{n}_0,m,l}(\vec{\rho}) \quad (11)$$

With

$$Y_0(\vec{\rho}) = \sum_{m=0}^{M-1}\sum_{l=0}^{L-1}\left|\hat{\psi}\left[a_{\min}a_0^m R(\frac{2\pi l}{L})\frac{2\pi}{\hbar}\vec{\rho}\right]\right|^2 \quad (12)$$

where $Y_0(\vec{\rho})$ is regularized for inversion by assigning $Y_0^{-1}(\vec{\rho}) = 0$ where $Y_0(\vec{\rho})$ drops below an appropriate threshold. The transform constitute a frame for a given image class $M$ if $\forall I \in M: Y_0(\vec{\rho}) = 0 \Rightarrow \hat{I}(\vec{\rho}) = 0$.

## IV. SHIFT INVARIANCE OF GABOR MAGNITUDES

We now argue that the magnitude of the Gabor wavelet transform is less sensitive to shift than the transform itself. Generally the amount of shift that can be tolerated by a representation is directly related to the frequency content of the underlying signal. For signals without band limitation (like Gabor-filtered images), the frequency content can be measured by the normalized frequency moments introduced by Dins Gabor (1946), who called them mean frequencies. The first one,

$$\vec{F}_1(f) = \frac{\int d^2\omega\vec{\omega}\left|\hat{f}(\vec{\omega})\right|^2}{\|f\|^2} \quad (13)$$

can be interpreted as the center of signal energy in the frequency space. For the Gabor function from equation (5) it is easily checked that $\vec{F}_1(\psi) \approx \vec{e}_1$ that is, any Gabor function is centered at the frequency that appears in the exponent of the first Gaussian in equation (3) (due to the admissibility correlation, this holds only approximately). For

non-pathological images, $\vec{F}_1(I*\psi) \approx \vec{e}_1$ will also holds, and for any real nonzero image, $\vec{F}_1(I*\psi) \approx \vec{e}_1$ must be different from $\vec{O}$. On the other hand, the Fourier transform of $|I*\psi|^2$ is the autocorrelation of $\hat{I}.\hat{\psi}$. Any autocorrelation is symmetric around the origin, and therefore $\vec{F}_1(I*\psi) \approx \vec{o}$. This argument shows that the magnitudes consist of lower frequencies and consequently show slower variation than the Gabor bands themselves. It can be looking at the second moment, the variance in frequency domain as well.

## V. RECONSTRUCTIONF ROM FOURIER MAGNITUDES

Due to their translation invariance, Fourier magnitudes have been used for pattern recognition [13]. The fact that the inverse DFT applied to modified transform with all magnitudes set to 1 and original phases preserves essential image properties [12] is frequently interpreted as saying that the Fourier magnitudes contain "less" image information than the phase. However, analytical results and existing phase retrieval algorithms provide hints the situation is not as simple. [14] show that the assumption of the global Fourier amplitude being irrelevant for the image contents is too simple although the amplitude spectrum averaged over orientations does not vary too much for natural images.

The possibility of reconstructing recognizable image from phase or amplitude information alone is not a contradiction to the above results. It only shows that it is very hard to trace the image information in the presence of the simplest of nonlinearities.

In the following we state some facts from [15,16] that show that almost all images can be reconstructed from their Fourier magnitude. The argument identifies unique reconstructability with the reducibility of a polynomial in D variables, where D is the signal dimension.

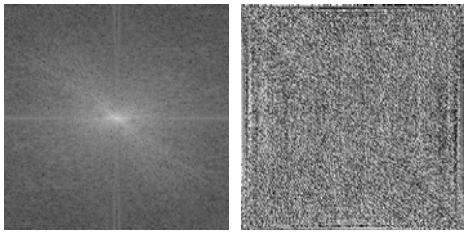

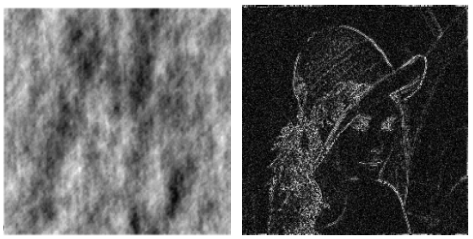

Fig. 1 In the top row is the original image. In the second row the original image was Fourier transformed, then split into the magnitude (left) and phase (right), and in the third row, the inverse Fourier transform of an arbitrarily chosen phase and the magnitude (left) and the opposite case in (right) are displayed respectively.

### A. Polynomials in One or More Dimensions

The set $P(n,D)$ of all polynomials with complex coefficients and total degree n in D variables is a vector over $C$ of dimension $\alpha(n,D)$. In the case $D=1$, all polynomials are reducible according to the fundamental theorem of algebra, that is, they can be factored into polynomials of lower degree for polynomials in two or more variables the situation is different the following is modified version from a theorem from [16] and shows that in certain sense, reducible polynomials are very uncommon in more than one variable.

*Theorem [1]*

The subset of polynomials in $P(n,D)$ that are reducible over the complex numbers corresponds to a set of measure zero in $R^{2\alpha(n,D)}$ provided $D>1$ and $n>1$ in the following sections we will make, full use of this result for two dimension signal processing the idea is that only images on a finite support are taken onto account and that the many wrong phase function lead to reconstructed images with non vanishing values outside this support. Throughout this paper we mean by a support of a function of two variables the smallest rectangle with edges parallel to the coordinate axis which contains all nonzero pixels. This should probably be a different name, but we don't expect any confusion by this simple terminology.

### B. Hayes Theorem and Extensions

Hayes's theorem identifies the 2D z-transform,

$$\hat{I}(\vec{z}) = \frac{1}{2\pi}\sum_{\vec{n}\in S_{\vec{N}}} I(\vec{n}) z_1^{-n_1} z_2^{-n_2} \tag{14}$$

and the 2D discrete space Fourier transform on a compact space support, with polynomials in two variables, to which theorem 1 applies.

*Theorem [2]*

Let $I_1, I_2$ be 2D real sequences support $S_{\vec{N}}$ and let $\Omega$ a set of $|\Omega|$ distinct points in $[-\pi,\pi]^2$ arranged on a lattice $L(\Omega)$ with $|\Omega| \geq (2N_1-1, 2N_2-1)$. If $\hat{I}(\vec{z})$ has

at most one irreducible nonsymmetrical factor and

$$\hat{I}_1(\nu) = \left|\hat{I}_2(\nu)\right| \forall\, \nu \in L(\Omega) \tag{15}$$

Then

$$\hat{I}_1(\vec{n}) \in \left\{I_2(\vec{n}), I_2(\vec{N}-\vec{n}-1), -I_2(\vec{n}), -I_2(\vec{N}-\vec{n}-1)\right\} \tag{16}$$

Theorem 2 states that DSFT magnitudes only reconstruction yields either the original, or a negated, point reflected, or a negated point reflected version of the input signal. Together with the statement of theorem 1 that the set of all reducible polynomials $\hat{I}(\vec{z})$ is of measure zero, the technicality about the irreducible nonsymmetric factors can be omitted, and we generalize theorem 2 to complex-valued sequences as follows

*Theorem [3]*

Let $I_1, I_2$ be complex sequences defined on the complex support $S_{\vec{N}}$ and let $\hat{I}_1(\nu)$ and $\hat{I}_2(\nu)$ be only trivially reducible and

$$\left|\hat{I}_1(\nu)\right| = \left|\hat{I}_2(\nu)\right| \forall\, \nu \in L(\Omega) \tag{17}$$

With $L(\Omega)$, $|\Omega|$ as in theorem 2. Then

$$I_1(\vec{n}) \in \left\{\exp(j\eta) I_2(\vec{n}), \exp(j\eta) I^*(\vec{N}-\vec{n}-1), \eta \in [0, 2\pi]\right\} \tag{18}$$

## VI. EXTENSION TO GABOR MAGNITUDE

Theorem 3 is a theorem about arbitrary polynomials; it can be applied equally well to magnitudes of a complex spatial image signal for reconstruction of the discrete Fourier transform.

*Theorem [4]*

Let $\mathrm{B}(N_1, N_2)$ be the space of all zero-mean band-limited functions on $S_{\vec{N}}$ such that $\hat{I}(\vec{\rho}) = 0$ for $\left|\rho_1 > \frac{N_1}{4}\right|, \left|\rho_2 > \frac{N_2}{4}\right|$ and $\hat{I}(0) = 0$ and let the wavelet family $\psi_{\vec{n}_0, m, l}(\vec{n})$ constitute a frame in $\mathrm{B}(N_1, N_2)$

For all $I_1, I_2 \in \mathrm{B}(N_1, N_2)$ such that

$\mathrm{I}_1(\vec{n}_0, m, l) = \langle I_1, \psi_{\vec{n}_0, m, l}\rangle$ and

$\mathrm{I}_2(\vec{n}_0, m, l) = \langle I_2, \psi_{\vec{n}_0, m, l}\rangle$

are only trivially reducible polynomials and

$$\left|\mathrm{I}_1(\vec{n}_0, m, l)\right| = \left|\mathrm{I}_2(\vec{n}_0, m, l)\right| \forall \vec{n}_0, m, l \tag{19}$$

it follows that

$$I_1(\vec{n}) = \pm I_2(\vec{n}) \tag{20}$$

*Proof*

From Plancherel's theorem, $\mathrm{I}_1(\vec{n}_0, m, l)$ is a polynomial:

$$\mathrm{I}_1(\vec{n}_0, m, l) = \sum_{\vec{\rho} \in S_{\vec{N}}} \hat{I}_1(\vec{\rho}) \frac{2\pi a_0^m}{\sqrt{N_1 N_2}\hbar^2} \hat{\psi}\left[a_{\min} a_0^m R\left(\frac{2\pi l}{L}\right)\frac{2\pi}{\hbar}\vec{\rho}\right] \exp(2j\pi n_0^T \vec{\rho}) \tag{21}$$

$I_1$ and $I_2$ are defined on $S_{\vec{N}}$ and their Gabor wavelet transforms are only trivially reducible polynomials in each sub-band $(m, l)$. For the frequency support argument, we shift the DFT frequency box so that $\vec{\rho} = \vec{0}$ is located in the middle of it. Then the support of both $I_1$ and $I_2$ becomes

$$\mathrm{T}_{\vec{K}} = \left\{\frac{-(K_1-1)}{2}, \ldots, \frac{(K_1-1)}{2} \times \frac{-(K_1-1)}{2}, \ldots, \frac{(K_1-1)}{2}\right\}$$

Since the images are real $K_1$ and $K_2$ must be odd numbers, and the support is symmetrical around $\vec{o}$. Furthermore, we define $\hat{\mathrm{I}}^s(\vec{\rho}, m, l)$ and as restricted of $\hat{\mathrm{I}}^s(\vec{\rho}, m, l)$ and $\hat{I}(\vec{\rho})$ on $\mathrm{T}_{\vec{K}}$

From the condition of the theorem, $N_1 \geq 2K_1 - 1, N_2 \geq 2K_2 - 1$

Thus

$$\left|\mathrm{I}_2(\vec{n}_0, m, l)\right| = \left|\mathrm{I}_1(\vec{n}_0, m, l)\right| \forall \vec{n}_0 \in S_{\vec{N}}, \forall m, l \Rightarrow$$
$$\hat{\mathrm{I}}^s(\vec{\rho}, m, l) \in \exp(j\eta(m, l))\hat{\mathrm{I}}_1^s(\vec{\rho}, m, l), \exp(j\eta(m, l))\hat{\mathrm{I}}_1^s(-\vec{\rho}, m, l) : \eta \in [0, 2\pi[ \tag{22}$$

That is, both Gabor transforms must be equal up to a phase and a possible point reflection, both of which may be depend on the sub-band. In the following steps, we remove the ambiguities exploiting known inter and intra sub-band structure in frequency domain. First we show that the magnitudes must be equal and the point reflected case cannot happen. Suppose

$$\left|\hat{\mathrm{I}}_2^s(\vec{\rho}, m, l)\right| = \left|\hat{\mathrm{I}}_1^{s*}(-\vec{\rho}, m, l)\right| \tag{23}$$

or equivalently,

$$\left|\hat{\mathrm{I}}_2^s(\vec{\rho}, m, l)\right| \left|\psi_{\vec{0}, m, l}(\vec{\rho})\right| = \left|\hat{\mathrm{I}}_1^s(\vec{\rho}, m, l)\right| \left|\psi_{\vec{0}, m, l}(-\vec{\rho})\right| \tag{24}$$

We pick a $\vec{\rho} \neq \vec{0}$, such that $\hat{\mathrm{I}}_1^s(\vec{\rho}) \neq \vec{0}$ and such that the angle between $\vec{\rho}_0$ and the kernel's center frequency is less than $\frac{\pi}{2}$. It can be concluded

$$\left|\psi_{\vec{0}, m, l}(\vec{\rho}_0)\right| > \left|\hat{\psi}_{\vec{0}, m, l}(-\vec{\rho}_0)\right| \tag{25}$$

Now, if we substitute $\vec{\rho}$ into equation 24, then equation 25 can be satisfied only if $\left|\hat{\mathrm{I}}_2^s(\vec{\rho}_0)\right| < \left|\hat{\mathrm{I}}_1^s(\vec{\rho}_0)\right|$ while substituting $-\vec{\rho}$ into equation 24 makes $\left|\hat{\mathrm{I}}_2^s(\vec{\rho}_0)\right| > \left|\hat{\mathrm{I}}_1^s(\vec{\rho}_0)\right|$ necessary. This is a contradiction. Second, we consider the Fourier phase in each sub-band:

$$\arg \hat{\mathrm{I}}_2^s(\vec{\rho}, m, l) = \eta(m, l) + \arg \hat{\mathrm{I}}_1^s(\vec{\rho}, m, l) \tag{26}$$

Because the phases of Gabor functions are equal for both images, it follows that

$$\arg \hat{\mathrm{I}}_2^s(\vec{\rho},m,l) = \eta(m,l) + \arg \hat{\mathrm{I}}_1^s(\vec{\rho},m,l) \quad (27)$$

except at the points where the Gabor function itself is zero, which are the grid points on the axis through $\vec{0}$ with the angle $\frac{2\pi}{L}(l+\frac{L}{2})$ .Applying equation 27 to a $\vec{\rho}_0$ and $-\vec{\rho}_0$ outside that axis and the zeros of $\hat{\mathrm{I}}_2^s$ yields, together with the fact that images are real

$$\eta(m,l) = 0 \ldots \eta(m,l) = \pi \quad (28)$$

Choosing any two combinations of $m,l$ there is always some points that lies on neither the exceptional axes and where the images is nonzero. Thus, $\eta(m,l)$ must be equal for those two levels, and consequently for all. This means that all sub-bands have the correct Fourier phase, or the phase function of all sub-bands has offset by $\pi$, and we conclude that

$$\hat{\mathrm{I}}_2^s(\vec{\rho}) = \pm \hat{\mathrm{I}}_1^s(\vec{\rho}) \quad (29)$$

From the band limitation in the conditions of the theorem, $\hat{\mathrm{I}}_1$ and $\hat{\mathrm{I}}_2$ are zero outside $\mathrm{T}_{\vec{K}}$

and therefore equation 29 also holds for them. Finally the inverse DFT yields

$$I_2(\vec{n}) = \pm I_1(\vec{n}) \quad (30)$$

which concludes the proof of the theorem.

## VII. RESULTS

In this section we explore the possibility of constructing a Gabor retrieval algorithm using the techniques from the proof of Theorem 4. We have interchanged spatial and frequency domain for the application of Hayes's Theorems, and the same can be done in the phase-retrieval algorithm. Then point reflections have been corrected with complex conjugation and the additive constant phase in each sub-band's frequency domain. The main problem in doing so is to make sure that the support covers all legal frequencies. The Gabor functions have no hard frequency bound, and the nonlinearity might introduce high frequencies in an unpredictable way. Reconstruction results 2 computed by the Gabor Retrieval algorithm. upper row: Original image, and in the bottom row result of the reconstruction after ten iterations from real, imaginary and absolute value respectively.

We have remarked that Gabor phase retrieval is a computational gamble, especially given the lack of convergence assertion even for the Fourier phase retrieval [17]. Furthermore, a complete Fourier phase retrieval for each sub-band is computationally expensive and provides poor results because the frequency images are not smooth enough see 1. So we decided to update the entire set of sub-band images by a support correction and after that to project these onto the range of the frame operator in order to get a legal Gabor wavelet transform. The extracted spatial phase functions are combined with the known space magnitudes in the next iteration. The support correction can be implemented by either of the following methods:

1. *Cutting of the sub-band frequency images at the frequency limit of the original image;*
2. *Attenuate the frequencies above the frequency limit;*
3. cutting out frequency circles containing the energy cluster at the expected location (For these experiments circular Gabor kernels have been used).

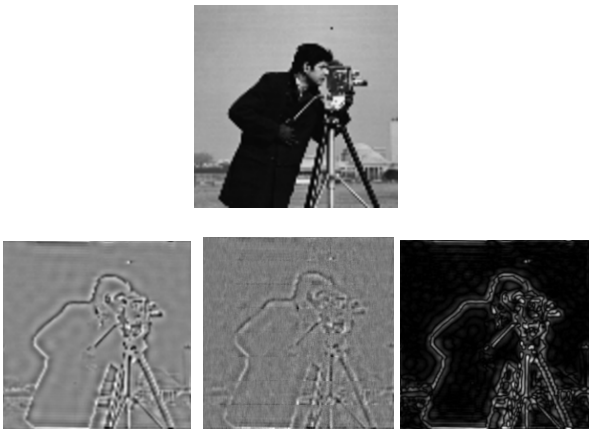

Fig. 2 In the top row is the original image. In the second row left reconstructed image after their real part, middle the reconstructed image from its imaginary part, and in the right the reconstructed image from their wavelet absolute value is displayed after 75 iterations

## VIII. CONCLUSION

We have shown that almost all images can be recovered from their Gabor magnitudes. As natural images, which are the only interesting ones for computer vision, constitute only a tiny subset of all functions with compact support, it is theoretically possible that many of them fall into the subset of images whose reconstruction is not unique, which we will call ambiguous. Although possible, this appears highly unlikely, because slight modifications of natural images still yield natural images. However, neither the set of natural images nor the precise form of the set of ambiguous images is known. The latter can not be uncovered with the simple dimensionality argument used in this paper and definitely requires further research. Furthermore, it is unclear how much the different reconstructions of ambiguous Gabor magnitudes will differ. If there should be two images with definitely different contents but nevertheless identical Gabor magnitudes, this would make the method problematic for image understanding. We have shown that this is very unlikely, but still have no absolute proof that it cannot happen. For further evidence, we have implemented a numerical algorithm for Gabor phase retrieval, which is based on the ideas of the proof. In the cases we tested, we could always recover a recognizable version of the image. A different reconstruction algorithm [4] uses gradient descent and also

yields very good results. Because Fourier phase retrieval algorithms cannot be proved to converge neither can ours. More detailed questions about, e.g., the sampling rate for numerically robust phase retrieval, remain open.

Our theorem suggests that twice the sampling rate is needed in each dimension for reconstruction from magnitudes only than for reconstruction from the full transform. As a simple rule of thumb, this looks very plausible in neuronal terms, if one considers a single complex number to be represented by four positive real numbers (because cell activities cannot be negative). Thus, four simple cells, which code for the linear wavelet coefficient, must be replaced by four complex cells at slightly different positions in order to convey the same information. However, it may still be suspected that a higher rate is necessary for numerical stability.

Finally, an efficient algorithm will probably not rely on separate phase retrieval for each of the many Gabor kernels contained in a frame but exploit the overlap (in frequency as well as in image space) of those kernels.

## ACKNOWLEDGMENT

The author would like to thank Christoph von der Malsburg and the developers of FLAVOR.

## REFERENCES

[1] J. Jones and L. Palmer , *An evaluation of two-dimensional Gabor filter model of simple receptive fields in cat striate cortex*, J. Neurophysiology 1987, pp.1233-1258.

[2] M. Lades, C. Vorbrüggen, J. Buhmann J. Lange C. von. der MalsburgR .P. Würtz, *Distortion Invariant Object Recognition in the Dynamic Link Architecture*, IEEE Transaction on computer, vol.42, number 3, 1993, pp.300-310.

[3] G. Kaiser, *Friendly Guide to Wavelets*, Birkhäuser, 1994.

[4] R. M. Farouk , *A system for Finding and segmenting a hand in Partially cluttered scene*, may 2007, Proceeding ICAS 29-31.

[5] J. G. Daugman *Uncertainty relation for resolution in space, spatial frequency, and orientation optimized by two-dimensional visual cortical filters*, Journal of the Optical Society of America vol. 2 number 7, 1985, pp. 1362-1373.

[6] D. A. Pollen, S. F. Ronner, *Phase relationships between adjacent simple cells in the visual cortex*, Science vol.212 , 1981, pp.1409-1411.

[7] C A. Daniel Steven F. Ronner, *Visual cortical neurons as localized spatial frequency filter*, IEEE Trans. on systems vol.38, number 2, 1992, pp. 587-607.

[8] R. M. Farouk, *Reconstruction of objects from images with partial occlusion*, PhD thesis 2006.

[9] I. Fogel D. Sagi, Gabor filters as texture *discriminator*, Biological Cybernetics, vol 16, 1989, pp.103-113.

[10] W. Xing B. Bhanu, *Gabor Wavelet Representation for 3-D Object Recognition*, IEEE Transactions on Image Processing vol. 6 number 1, 1997, pp.47-64.

[11] L. Shen L. Bai M. Fairhurst, *Gabor wavelets and General Discriminant Analysis for face identification and verifications*, J. Image vision computing vol. 25, 2007, pp. 553-563.

[12] G. Xijin S. Iwata, *Learning the parts of objects by Auto-association*, vol.15, 2002, pp.285-295.

[13] P.H. Gardenier , B.C. McClellan R. H. T. Bates, *Fourier transform magnitudes are unique pattern recognition templates*, Biological Cybernetics vol. 54 pp.385-391 1986.

[14] M. Nabti A. Bouridane, *An effective and fast iris recognition system based on a combined multiscale feature extraction technique*, Pattern Recognition vol. 41 2008.

[15] M.H. Hayes , *The reconstruction of a multidimensional sequence from the phase or magnitude of its Fourier transform*, IEEE Trans. on Acoustics, speech, and Signal Processing vol. 30 number 2 , pp.140-154 1982.

[16] M. H. Hayes H. J. McClellan, *Reducible polynomials in more than one variable*, Proceeding of IEEE vol.70 number 2 pp. 197-198 1982.

[17] J. R. Fienup, *Reconstruction of complex-valued object from the modulus of its Fourier transform using a support constraint*, J. of Optical Society of America vol.4 number 1 pp. 118-123 1987.